Aerosol and Air Quality Research

ORIGINAL RESEARCH
https://doi.org/10.4209/aaqr.210251

Adsorption and Decomposition of NO_x on Heteropolyacids: An Evaluation of the Adsorption Performance

Hongjian Zhu[1], Meiqing Yu[1], Tao Ma[1], Rui Wang[1,2*], Korchak Vladimir[3], Vladimir N. Korchak[3], Vitaly Edwardovich Matulis[4]

[1] School of Environmental Science and Engineering, Shandong University, Qingdao 266237, China
[2] Shenzhen Research Institute of Shandong University, Shenzhen 518057, China
[3] Laboratory of Heterogeneous Catalysis, Semenov Institute of Chemical Physics, Russian Academy of Sciences, Moscow 119991, Russian Federation
[4] Laboratory of Chemistry of Condensed Matter of the Scientific-Research Institute for Physical-Chemical Problems, The Belarusian State University, Minsk 220006, Republic of Belarus

ABSTRACT

In order to develop an efficient method by which to eliminate NO_x pollution, several new catalyst systems including different heteropolyacids (HPAs) and supported phosphotungstic acids (HPWs) (HPW/SiO_2, HPW/SnO_2, HPW/USY and HPW/ZSM-5) for adsorption-decomposition of NO_x were prepared and studied. The obtained catalysts were characterized using Brunauer-Emmett-Teller (BET) measurement and Fourier transform infrared (FT-IR) analysis. The results showed that W-containing HPAs were superior to Mo-containing HPAs. Among the selected catalysts, HPW/SnO_2 with a 50% HPW loading had the highest NO_x adsorption rate of 77.3%, for which the amount of saturated NO_x adsorption (85.4 mg g^{-1}) was much higher than that of HPW (50.5 mg g^{-1}). The NO_x adsorption performance of the catalyst was mainly determined by the interaction between the support and the HPW, which was also affected by the specific surface area of the catalyst. FTIR characterization revealed that the adsorbed NO_x mainly existed in the HPW bulk phase in the form of NOH^+. A gas chromatograph-mass spectrometer (GC-MS) was used to confirm the effectiveness of NO_x decomposition into N_2.

Keywords: Polyoxometalate, NO_x, Adsorption, Decomposition, Support

Received: September 22, 2021
Revised: November 13, 2021
Accepted: November 16, 2021

* **Corresponding Author:**
wangrui@sdu.cn

Publisher:
Taiwan Association for Aerosol Research
ISSN: 1680-8584 print
ISSN: 2071-1409 online

1 INTRODUCTION

NO_x (NO and NO_2) are major air pollutants derived from stationary power sources and mobile sources that not only are extremely toxic to human body, but also can lead to photochemical smog, acid rain, ozone depletion, and the greenhouse effect (Liu *et al.*, 2014; Jiang *et al.,* 2016; Huang *et al.*, 2019). Alternative well-developed technologies have been employed for eliminating NO_x emissions in response to environmental protection requirements. Among them, selective catalytic reduction of NO_x with NH_3 (NH_3-SCR) has been considered to be one of the most efficient techniques for NO_x removal due to its efficiency, economy, and selectivity (Forzatti *et al.*, 2009; Imanaka and Masui, 2012). However, the leakage of ammonia can cause secondary pollution. The catalytic decomposition of NO_x has attracted much attention because it can directly decompose NO_x into N_2 and O_2 without consuming any reducing agent, and the operation process is simple, economical, and without secondary pollutants. In recent years, various catalysts, including precious metals, metal oxides, ion exchange molecular sieves, perovskite-type composite oxides and carbonitrides (Konsolakis and Michalis, 2014; Sun *et al.,* 2014), have been used in direct decomposition of NO_x under high temperature conditions ($> 500°C$).

Polyoxometalates (POMs) have been used in a variety of catalytic fields owing to their strong

Brønsted acidity, remarkable redox properties, and pseudo-liquid phase behavior (Wang and Yang, 2015; Ren *et al.*, 2017a, b). In particular, HPAs have shown attractive NO_x adsorption performance and can decompose the adsorbed NO_x into N_2 through rapid heating. Yang and Chen (1994; 1995) reported that NO_x was adsorbed on HPW in the form of protonated NO (NOH^+), and N-O cleavage was generated in the rapid heating process, thus resulting in N_2 yield. However, the small specific surface area and low mechanical strength of HPA and its inferior thermal stability makes it difficult to reuse in practical applications. Therefore, many supported HPA materials have been developed to improve its adsorption performance, catalytic decomposition activity, and stability. In representative lean-gas mixture conditions, the NO_x storage and reduction performance of $H_3PW_{12}O_{40}{\cdot}6H_2O$ loaded on Ti-Zr and Ce-Zr mixed oxides were studied and shown to have high N_2 selectivity (Gómez-García *et al.*, 2005a, b). Platinum (Pt) and HPW doped mesoporous MSU-type silica mixtures were used for NO_x adsorption (Hamad *et al.*, 2007). HPW/CNTs catalysts were prepared, and the results showed that the yield of N_2 after microwave heating was higher than that obtained with rapid heating using a resistance furnace (Zhang *et al.*, 2012). Zhang *et al.* (2013) designed a new HPW-USY catalyst with a three-dimensional ship-in-bottle structure. It had high thermal stability and good NO_x decomposition performance. In principle, the materials with an isoelectric point of 7 generally do not affect the structure and chemical properties of HPA, which are suitable as HPA supports. A new Keggin-type HPA, germanium-based HPA ($H_4GeW_{12}O_{40}$) was synthesized and utilized as a catalyst for removal of NO_x. The results demonstrated a NO_x removal rate of 81.5% and N_2 selectivity of 68.3% (Wang *et al.*, 2021). $H_3PW_{12}O_{40}$ (HPW)-modified Fe_2O_3 catalysts were synthesized for the selective catalytic reduction of NO_x by NH_3 (NH_3-SCR). The optimum HPW/Fe_2O_3-350-0.5 catalyst exhibited nearly a 100% NO conversion at 240–460°C as well as excellent SO_2 resistance (Wu *et al.*, 2021). The NO_x adsorption performance of the catalyst determines the amount of NO_x decomposed. The development of catalysts with high activity and stability have consistently been a research hotspot and have been proven to be quite challenging. The factors affecting the adsorption performance of catalysts also require further exploration.

The objective of this work is to develop a novel, economical, and environmentally friendly NO_x conversion catalyst and to further understand the constraints that affect catalytic performance. In this work, various HPAs and supported HPW (HPW/SiO_2, HPW/SnO_2, HPW/USY and HPW/ZSM-5) were prepared and used for the adsorption and decomposition of NO_x. The physical and chemical properties of the catalyst were characterized using BET and FTIR spectra. The relationship between their NO_x adsorption performance and their physicochemical properties was analyzed through comparative studies.

2 EXPERIMENTAL PROCEDURE

2.1 Materials

Commercial heteropolyacids, including $H_3PW_{12}O_{40}$ (HPW), $H_4SiW_{12}O_{40}$ (HSiW), $H_3PMo_{12}O_{40}$ (HPMo), $H_4SiMo_{12}O_{40}$ (HSiMo) and SnO_2, were obtained from Sinopharm Chemical Reagent Co., Ltd (China). SiO_2 was purchased from Alfa Aesar. USY and ZSM-5 molecular sieves were purchased from the Zhoucun Catalyst Factory and Jiangsu Aoke Petrochemical Science and Technology Company. All reagents were analytical grade and were used directly without further purification.

2.2 Synthesis of HPW-Loaded Materials

HPW-loaded materials were prepared using the impregnation method. The mass ratios of HPW/(HPW + support) were 0, 16.7%, 28.6%, 37.5%, 44.4%, and 50.0%. A specific mass ratio of the support was immersed in a quantitative HPW solution for 24 h and then dried in a 60°C water bath for 1 h to obtain the samples. The samples were denoted as HPW/SiO_2, HPW/USY, HPW/SiO_2, and HPW/ZSM-5.

2.3 Catalyst Characterization

FTIR spectra of the samples were recorded using a Nicolet Avatar370, and the spectral domain ranged between 400 and 4000 cm^{-1} at a 4 cm^{-1} resolution. The BET surface areas of the catalysts were measured based on the N_2 adsorption at –196°C using a Micromeritics ASAP 2010 apparatus.

2.4 Activity Tests

2.4.1 Standard test procedure: Adsorption stage

The experiments were carried out in a fixed-bed quartz tube reactor (inner diameter = 8 mm). 0.3 g of the sample was placed in the middle of the reactor between two quartz wool plugs and pretreated with highly purified N_2 at 150°C for 1 h. During NO_x adsorption, the feed gas containing 800 ppm NO, 8% O_2, 4.2% H_2O, and balance He was passed through a bench blending reactor and partially converted to NO_2 ($2NO + O_2 = 2NO_2$), yielding an NO_x mixture. NO and NO_2 analyzers (TH-990S) were used to continuously record the concentration at the NO and NO_2 outlet.

The NO_x adsorption amount in terms of NO_2 was calculated by integrating the curve below the baseline (1000 ppm) and expressed in mg g^{-1}. The calculation formula is shown below:

$$M = \frac{Q\int_0^t Cdt}{m}, \tag{1}$$

where m represents the mass of the catalyst (g); Q is the total gas flow (m^3 min^{-1}); C is the NO_x removal concentration (mg m^{-3}), and t is the adsorption time (min).

2.4.2 Decomposition stage

After NO_x adsorption saturation, the reactor containing the catalyst was purged with He flow (5 mL min^{-1}) for 1 h. Then, the reactor was placed in a tube furnace and rapidly heated from 30°C to 450°C at a heating rate of 150°C min^{-1}. The decomposition product was detected with a GC-MS analyzer.

NO conversion was then calculated using the following formula:

$$N_2\ (\text{yield}) = \frac{2N_2\ (\text{formation})}{NO_x\ (\text{adsorbed})} \times 100\% \tag{2}$$

where NO_x (adsorbed) represents the amount of HPW the NO_x adsorbed, and N_2 formation represents the amount of N_2 generated during NO conversion.

3 RESULTS AND DISCUSSION

3.1 FTIR Analysis

FTIR spectra are the most commonly used research and measurement method applied to polyanions. The FTIR spectra of the supports before and after loading with HPW are shown in Fig. 1(a–d), and the FTIR spectrum of the HPW used in this work is shown in Fig. 1(e). Four characteristic peaks of the Keggin structure can be observed at 1080 cm^{-1}, 983 cm^{-1}, 892 cm^{-1}, and 801 cm^{-1}, corresponding to P-O_a, W = O_d, W-O_b-W, W-O_c-W, respectively, which is consistent with the literature (Yang and Chen, 1994). As shown in Fig. 1(a), for HPW/SiO_2, the P-O_a absorption peak of HPW at 1080 cm^{-1} became broader due to being masked by a wide SiO_2 absorption peak at 1086 cm^{-1}. The other three absorption peak positions of HPW shifted slightly, and their peak intensity decreased significantly. These findings implied that the HPW Keggin structure still existed after loading HPW on SiO_2. The change in the characteristic peaks indicated that an interaction between HPW and SiO_2 occurred. The negative charge of the heteropolyanion increased after the HPW was loaded on SiO_2, where the increased negative charge could fill its antibonding molecular orbital, leading to a reduction in the chemical bond strength and a decrease in the vibration frequency.

In Fig. 1(b), a broad peak can be observed at 400–750 cm^{-1} (650 cm^{-1}), which was mainly attributed to the stretching vibration of the Sn-O band (Abello *et al.*, 1998; Singh *et al.*, 2014). When comparing the IR spectra of SnO_2 and HPW/SnO_2, it can be seen that the four characteristic peaks of the Keggin structure on HPW/SnO_2 were stable, indicating that HPW was definitely loaded on the SnO_2, and there was no strong interaction between the SnO_2 and the HPW, thereby preserving the heteropolyanion phase.

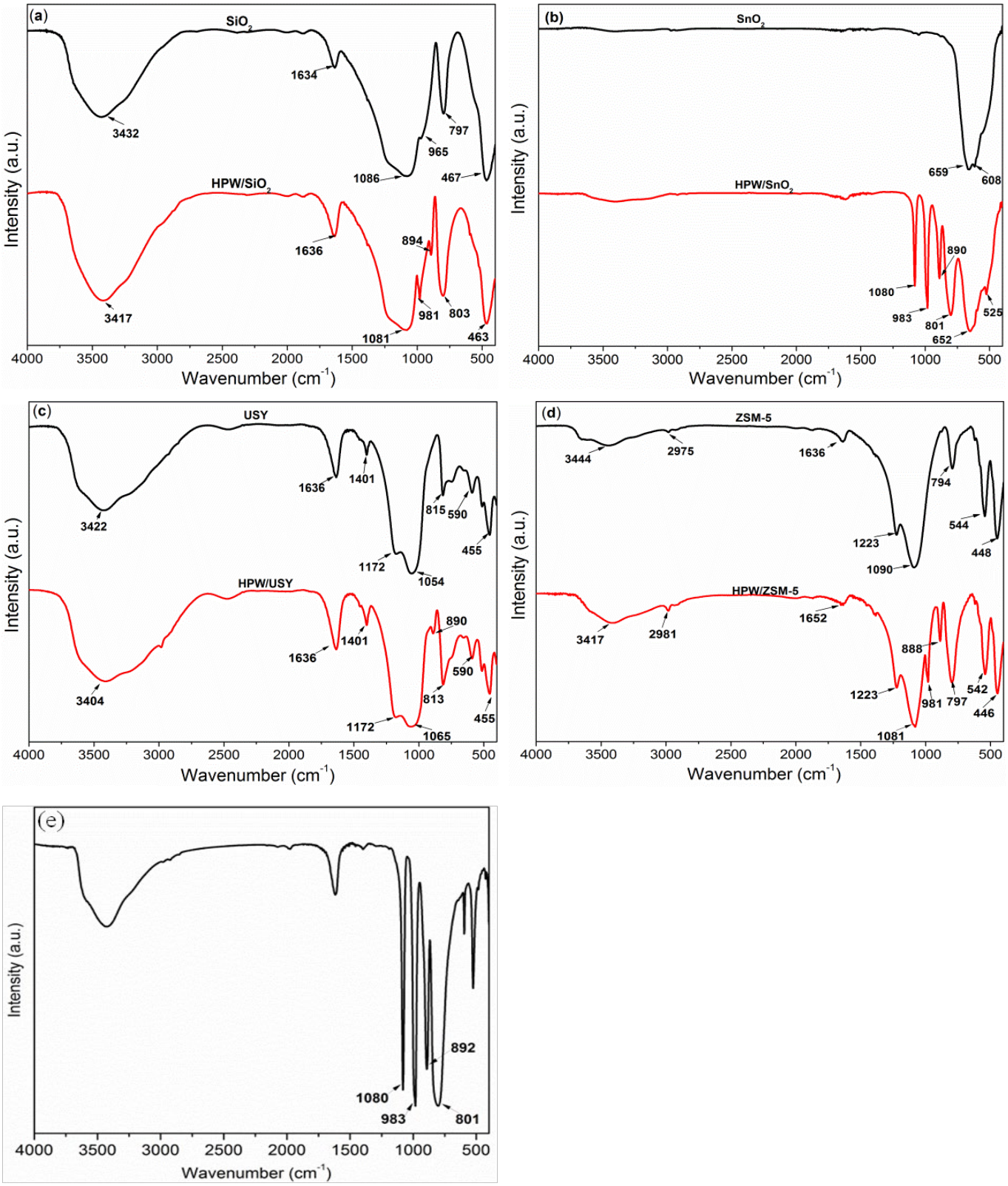

Fig. 1. FTIR spectra of HPW and various supports with a 50% HPW loading.

As shown in Fig. 1(c), the USY framework structure can be identified by the peaks at 1700–400 cm^{-1} (Zhang *et al.*, 2001; Munir and Usman, 2018). The absorption band at 1636 cm^{-1} was assigned to the bending vibration of the -OH group. The broad band from 1000 to 1250 cm^{-1} represented the asymmetric stretching vibration of Si-O-Si. The absorption bands at 815 cm^{-1}

and 455 cm^{-1} were attributed to the bending vibration of Si-O-Si. In addition, a band at 590 cm^{-1} was observed, indicating the presence of a zeolite framework with tetrahedral units of SiO_4 and AlO_4. The characteristic peak of the of USY continued to exist on HPW/USY, indicating that the cage-type micropore structure of USY was preserved, and the strong interaction between USY and HPW caused the characteristic peak of the zeolite to shift. The broader absorption peak of USY at 1054 cm^{-1} covered the P-O_a band and the HPW W = O_d band. The W-O_b-W band and the W-O_c-W band shifted slightly, and their peak intensity was greatly reduced or even disappeared. This indicated that the Keggin structure in HPW/USY basically existed, but the strong interaction between HPW and USY may have deformed the PO_4 tetrahedral structure in the heteropolyanion and weakened W-O bond outside the heteropolyanion structure.

Fig. 1(d) shows the IR spectrum of HPW/ZSM-5. The peaks appearing at 1223 cm^{-1}, 1090 cm^{-1}, 794 cm^{-1}, 544 cm^{-1}, and 448 cm^{-1} can be ascribed to the typical characteristic peaks of a ZSM-5 molecular sieve framework (On *et al.*, 1995; Shirazi *et al.*, 2010). In the case of HPW/ZSM-5, the characteristic peak of the ZSM-5 framework structure and the HPW Keggin structure can be found with a weak deviation. Therefore, HPW/ZSM-5 not only maintained the porous zeolite structure of ZSM-5, but also the HPW Keggin structure on ZSM-5 was not destroyed, indicating that the interaction between HPW and ZSM-5 was relatively small, which was similar to HPW/SnO_2. The combination of the characteristics of HPW and the support was more conducive to the improvement in the deNO_x performance.

3.2 BET

Table 1 lists the specific surface area of the four catalyst systems with the preferred HPW loading. The specific surface area of HPW was only 3.2 $m^2\ g^{-1}$. For the supports, an obvious difference in specific surface area was observed. The specific surface areas of SiO_2, SnO_2, USY, and ZSM-5 were 334.2 $m^2\ g^{-1}$, 10.4 $m^2\ g^{-1}$, 559.8 $m^2\ g^{-1}$, and 305.4 $m^2\ g^{-1}$, respectively. In general, for adsorption reactions, a larger specific surface area is beneficial in terms of providing more adsorption sites, thereby improving the adsorption performance of the catalyst. Actually, it can be found that for all supports loaded with HPW, as the HPW loading increased, the specific surface area of the sample gradually decreased to varying degrees. This indicated that the HPW was effectively loaded on the supports, and the interaction between the highly dispersed HPW and the supports had an inhibiting effect in specific surface areas.

3.3 Adsorption Performance of Heteropoly Acids for NO_x

The NO_x adsorption performance of four heteropoly acids (HPW, HSiW, HPMo, and HSiMo) was investigated. As shown in the Fig. 2, during the experimental period, relatively stable adsorption rates were observed on the four heteropoly acids. The NO_x adsorption rates after a 40 min reaction time with HPW, HSiW, HSiMo, and HPMo were 66.5%, 62.9%, 30.7%, and 24.4%, respectively. Among the four heteropolyacids, HPW showed the best NO_x adsorption performance. From the

Table 1. NO_x adsorption rate and the specific surface area of the various samples.

Samples	Loading amount	BET ($m^2\ g^{-1}$)	NO_x adsorption rate
HPW	100%	3.2	66.5%
SiO_2	0	334.2	35.2%
HPW/SiO_2	28.6%	236.5	62.3%
HPW/SiO_2	50%	135.8	50.9%
SnO_2	0	10.4	13.7%
HPW/SnO_2	37.5%	9.2	70.1%
HPW/SnO_2	50%	6.5	77.3%
USY	0	559.8	48.3%
HPW/USY	16.7%	535.2	65.7%
HPW/USY	50%	245.2	38.3%
ZSM-5	0	305.4	27.7%
HPW/ZSM-5	28.6%	223.1	57.6%
HPW/ZSM-5	50%	170.6	70.5%

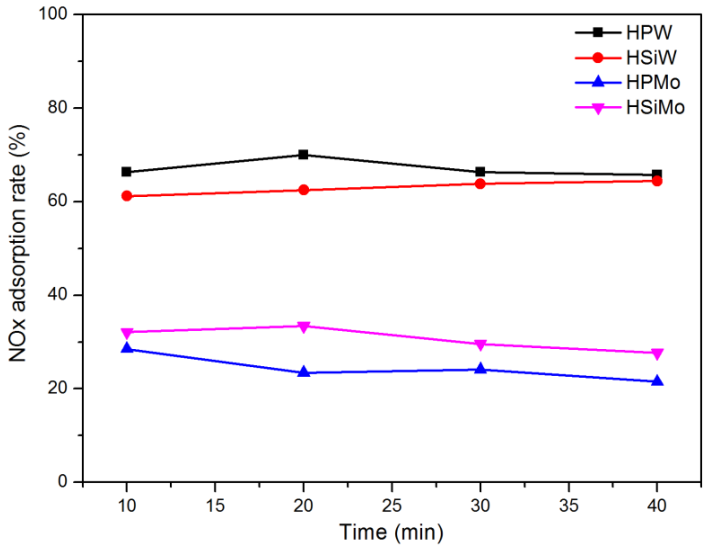

Fig. 2. NO_x adsorption performance of HPW, HSiW, HSiMo and HPMo.

experimental results, the NO_x adsorption rates of the W-containing heteropolyacids (HPW and HSiW) were much higher than that of Mo-containing heteropolyacids (HSiMo and HPMo), indicating that the NO_x adsorption performance of heteropolyacid could be closely related to the composition of its anions, especially the type of coordination atoms in the anions. This result was consistent with the conclusion of Belanger and Moffat (1995). Indeed, the acid strength of the W-based heteropolyacids was higher than that of the Mo-based heteropolyacids (Jozefowicz *et al.*, 1993). It can be inferred that the NO_x adsorption rates of the four heteropolyacids were correlated with their acid strengths.

3.4 Effect of HPW Loading on NO_x Adsorption for Various Supports

NO_x adsorption experiments were carried out on various supports with different HPW loading amounts. The NO_x adsorption rate was plotted as a function of the adsorption time reached by each catalyst in the NO-TPO experiment (Fig. 3). These results were derived as shown in Fig. 4 in order to better compare the effect of different HPW loading amounts on the NO_x adsorption performance of the catalyst. As shown in Fig. 4(a), the loading amounts of HPW were 0, 16.7%, 28.6%, 37.5%, 44.4%, and 50.0%, for which the corresponding NO_x adsorption rates of HPW/SiO_2 were 35.2%, 39.6%, 62.3%, 56.6%, 49.3%, and 50.9%, respectively. It was found that the NO_x adsorption performance of pure SiO_2 was very low. After loading with HPW, the NO_x adsorption efficiency of the catalytic system increased immediately. When the HPW loading exceeded 30%, the NO_x adsorption efficiency of HPW/SiO_2 decreased steadily with increases in the loading, but it was still higher than the performance of the pure SiO_2. The best deNO_x performance was obtained when the HPW loading was 28.6% for the HPW/SiO_2 system. The NO_x adsorption rate for HPW/SnO_2 is shown in Fig. 4(b). Pure SnO_2 exhibited an extremely low NO_x adsorption rate (13.7%), where after a small amount of HPW was loaded, the NO_x adsorption performance increased sharply. The deNO_x performance of HPW/SnO_2 basically increased with increases in the amount of loaded HPW, but the performance decreased slightly at 37.5% and then rebounded again. It should be noted that the NO_x adsorption rate of HPW/SnO_2 with a 50% HPW loading amount reached 77.3%. Fig. 4(c) shows the NO_x adsorption rate of HPW/USY. HPW/USY exhibited a similar trend to that of the HPW/SiO_2 system; that is, the NO_x adsorption rate increased first and then decreased with increases in the HPW loading amounts. For HPW/USY, the optimal HPW load was 16.7%. Fig. 4(d) shows the NO_x adsorption rates of HPW/ZSM-5 corresponding to HPW loadings of 0, 28.6%, 37.5%, 44.4% and 50% were 27.7%, 57.6%, 62.6%, 65.2% and 70.5%, respectively. The results showed that as the HPW loading amount increased, the NO_x adsorption performance of HPW/ZSM-5 increased steadily. This may have been due to the fact that the ZSM-5 is a molecular sieve material with a large specific surface area and a rich pore structure. The heteropoly acid loading can cause the specific surface area and pores to decrease, but it does not

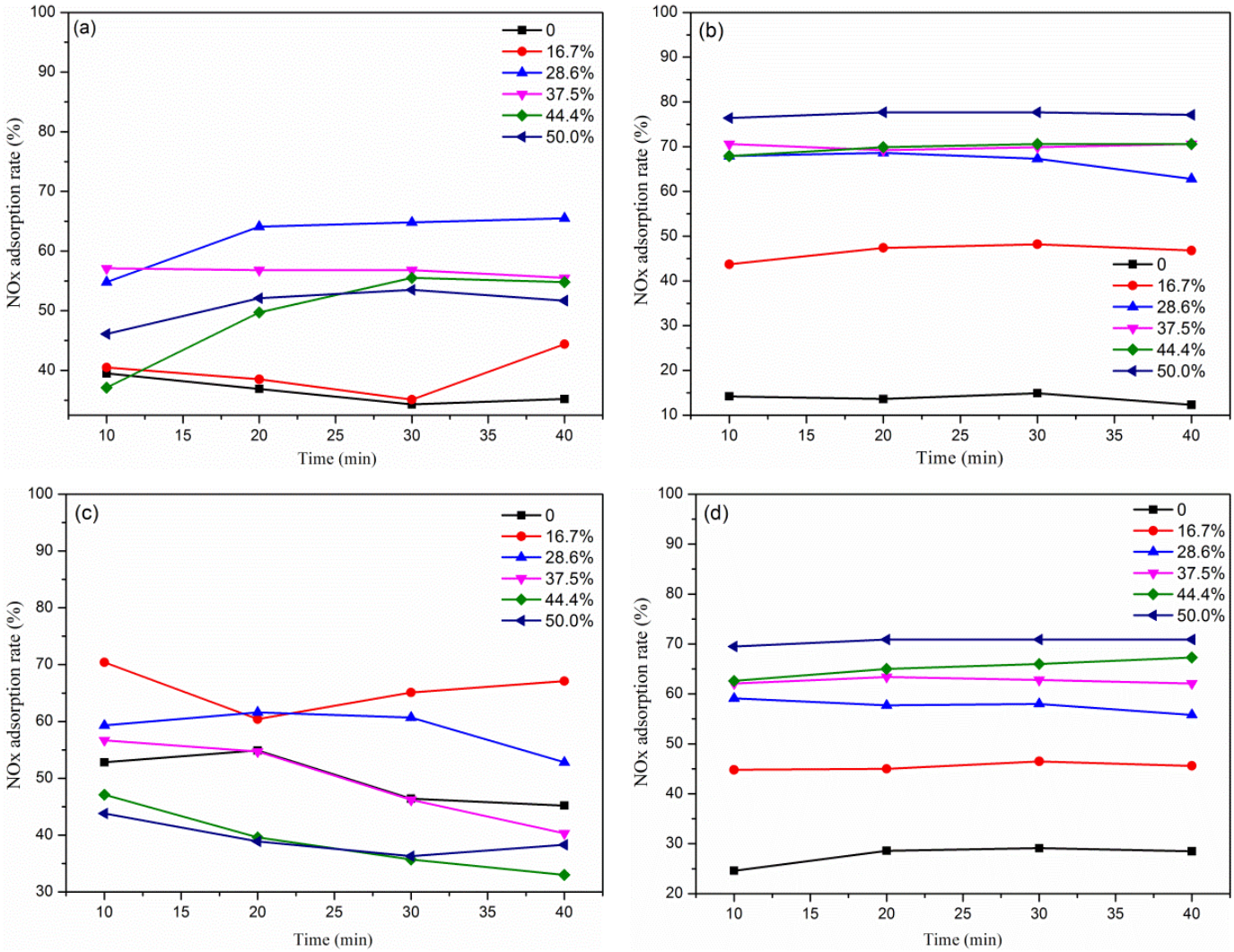

Fig. 3. NO_x adsorption performance of various supports with different HPW loading amounts. (a) HPW/SiO_2, (b) HPW/SnO_2, (c) HPW/USY, and (d) HPW/ZSM-5.

lead to the destruction of the structure. Thus, a synergistic effect on the NO_x adsorption performance was observed.

Comparing the four sets of data, it was found that the adsorption curve showed two different changes, which was a meaningful for determining the nature of the NO_x adsorption. When unloaded supports were used for NO_x adsorption, their adsorption rate sequences were USY > SiO_2 > ZSM-5 > SnO_2, which was consistent with their specific surface area sequence, indicating that a specific surface area plays a certain role in NO_x adsorption. When SiO_2 and USY were used as the HPW supports for NO_x adsorption, the basic trend in the adsorption performance indicated similar volcanic changes. It can be seen that the highest NO_x adsorption rates of HPW/SiO_2 and HPW/USY were 62.4% and 65.6%, respectively, both still slightly lower than that of pure HPW (66.5%), which meant that HPW was the main active component leading to NO_x adsorption. According to the BET data, the increased HPW loading on SiO_2 and USY caused a significant decrease in their specific surface area. For HPW/SiO_2 and HPW/USY with the 50% HPW loading, the specific surface area decreased by 59.3% and 56.1%, respectively, compared to the pure supports. The high loading amount made it possible for a significant amount of HPW to enter the support pores, which blocked its porous passages or collapsed the microporous structure, leading to a reduction in the specific surface area. After the highly dispersed HPW was wrapped in the pores of the support, it may have instead reduced the probability of contact between the HPW body phase and reactive molecules, thus limiting the HPW-specific pseudo liquid phase behavior.

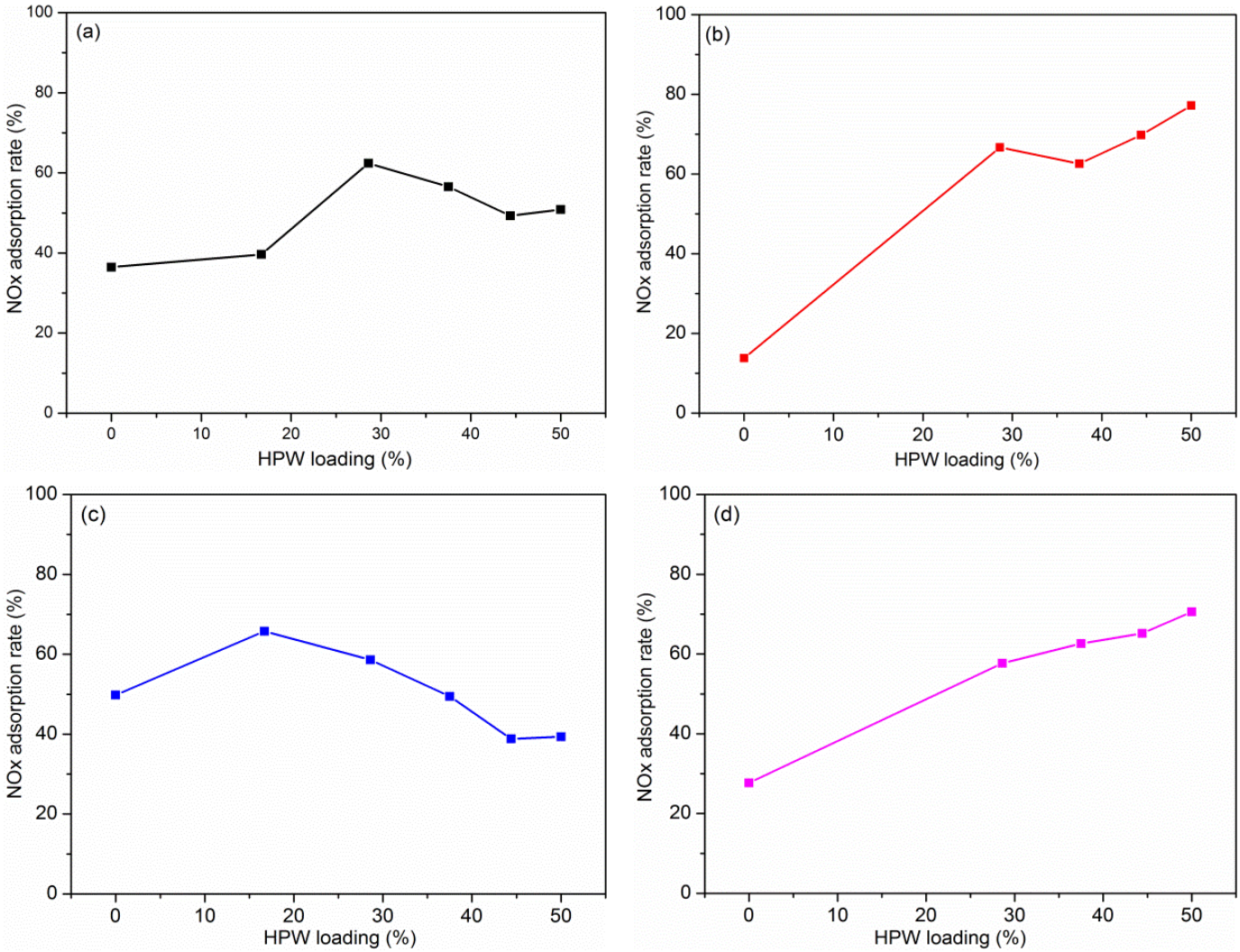

Fig. 4. Effect of HPW loading on NO_x adsorption for various supports (a) HPW/SiO_2, (b) HPW/SnO_2, (c) HPW/USY, and (d) HPW/ZSM-5. Reaction conditions: 800 ppm NO, 8% O_2, 4.2% H_2O, T = 150°C, SV = 10580 h^{-1}.

This may be one reason for the initial increase in the deNO_x performance of HPW/SiO_2 and HPW/USY and the subsequent decrease with HPW loading. In addition, the strong interaction between HPW and the surface properties (hydroxyl groups and acid sites) of the support was an important factor affecting the deNO_x performance. After loading, the HPW acid amount and acid type remain unchanged, but the acid strength decreased, and the degree to which the acid strength was decreased was also related to the strength of the surface interaction, where a stronger surface interaction led to the lower acid strength. Rocchiccioli-Deltcheff *et al.* (2010) believed that the effect of HPW and hydroxyl groups on the surface of SiO_2 would cause the acidity and redox of the heteropoly acid to decrease at the same time, thereby leading to reduced catalytic performance. Mccormick *et al*. (1998) also reported that HPW interacts strongly with the hydroxyl groups on the surface of the SiO_2 support, resulting in a completely different secondary structure from HPW.

For HPW/USY, there was a strong interaction and a weak interaction between the HPW and the silicon hydroxyl group (Si-OH) on the surface of USY, respectively, where the strong interaction consumed H^+ to produce water, and the weak interaction caused a H^+ transfer (Liu *et al.*, 2003). Indeed, there were various hydroxyl groups on the surface of the USY channel, including surface Si-OH, skeleton surface Al-OH, and non-framework Al-OH, so the source of acidity of HPW/USY was more complicated. HPW may also interact weakly with the abundant Si-OH in the hydroxyl socket of the USY secondary pore, resulting in a decrease in the acid strength. In addition, the

acid-base interaction between the Al species in the USY and HPW may have decreased the acid strength. The decrease in the total acid content on HPW/USY with a high HPW loading may have been due to the decreased surface area of the catalyst, which led to a reduction in the available surface acid centers, thereby reducing the adsorption performance of the catalyst. ZSM-5 and USY are both zeolite molecular sieves with a Si-Al framework structure. However, they have different frameworks, pore structures, and surface properties. It is clear that the specific surface area of HPW/ZSM-5 from pure ZSM-5 to the 50% loading was only decreased by 44.1%, which indicated that the negative effect of increasing the HPW loading amount and the clogging of the carrier pores was less than that in the case of USY. Furthermore, the amount of non-framework Al remaining in the pores of ZSM-5 may have been much less than that in USY (Shen *et al.*, 2007), which reduced the probability of non-framework Al damaging the acidic center of the HPW with a Keggin structure. Thus, the NO_x adsorption rate and the trend of the changes in the deNO_x performance with the HPW loading amount were obviously different. It is worth noting that SnO_2 was completely different from the other conventional supports in terms of interacting with HPW to participate in NO_x adsorption. Conventional porous supports generally rely on their own excellent pore structure and high specific surface area to efficiently disperse HPW active centers to facilitate the entry of NO_x molecules into the HPW body. However, the specific surface area of SnO_2 is very small and clearly does not have the properties characteristic of porous materials. In addition, SnO_2 is a semiconductor material with a specific concentration of oxygen vacancies. It has thus been speculated that SnO_2 can be used as a high-efficiency catalytic promoter in the place of ordinary supports. Zhang *et al*. (2002) studied the desorption and decomposition of NO by HPW/TiO_2 and speculated the trapping effect of oxygen vacancies on the surface of TiO_2. O_2 is essential in the process of HPW adsorption of NO_x. The doping of SnO_2 can increase the O_2 adsorption capacity of the catalyst surface in the NO_x adsorption process. Therefore, this combination can demonstrate significantly increased NO_x adsorption capacity through synergistic effects that occur between SnO_2 and HPW, where HPW/SnO_2 with the 50% loading had the best deNO_x performance.

3.5 Adsorption Capacity

Adsorption capacity is an important indicator to evaluate the performance of an adsorbent. The NO_x saturation adsorption curves for HPW and HPW/SnO_2 with a 50% HPW loading amount at 150°C were investigated, as shown in Fig. 5. The calculated saturation adsorption capacity of HPW was 50.5 mg g^{-1}. The NO_x saturation adsorption capacity of HPW/SnO_2 was equivalent to 85.4 mg g^{-1}, which was higher than that of Ti-Zr (28 mg g^{-1}) and TiO_2 (46 mg g^{-1}) as supports reported in the previous literature (Hodjati *et al.*, 2001; Gómez-García *et al.*, 2005b). It was thus found that the amount of HPW used was reduced, and the stability of the catalyst increased

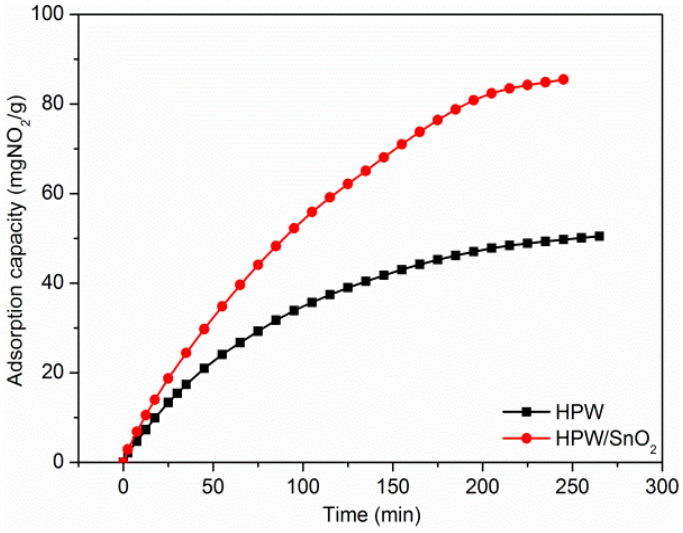

Fig. 5. The saturation adsorption capacity of HPW and HPW/SnO_2 (50% loading).

after the HPW was supported on SnO_2. Furthermore, this combination still maintained excellent NO_x adsorption performance.

3.6 Adsorption Mechanism

In this experiment, the HPW and HPW/SnO_2 samples after adsorption saturation were characterized using FTIR, as shown in Fig. 6. It can be observed that four characteristic peaks of the Keggin structure still existed in the range of 700–1100 cm^{-1}, indicating that the two samples maintained a stable Keggin structure after being saturated with NO_x. In addition, a new characteristic peak appeared at 2266 cm^{-1} for the two samples. Yang and Chen (1994, 1995) carried out IR characterization of pure HPW saturated with NO_x and found an absorption peak at 2270 cm^{-1}. According to TGA and the calculation of the mass conservation principle of nitrogen, the absorption peak at 2270 cm^{-1} was regarded as ionic protonated NO (NOH^+). Thus, a classic NO adsorption mechanism was proposed where the adsorbed NO was retained in the bulk HPW phase in the form of NOH^+ by replacing the crystal water in HPW. Herring *et al.* (1998, 2010) improved the NO adsorption mechanism and confirmed that the protons existed in the secondary structure of heteropoly acid in the form of H_3O^+ or $H_5O_2^+$. Particularly, protonated water was a prerequisite for NO to enter the HPA secondary structure and exist as NOH^+.

According to the above analyses, the vibration peak at 2266 cm^{-1} detected in this experiment could be ascribed to NO^+. Furthermore, the characteristic bending vibration peaks of NO_2^+ (570 cm^{-1}) were not detected. The HPA used in this work was $H_3PW_{12}O_{40}{\cdot}6H_2O$. At most, 6 crystal water molecules could be replaced in one HPW molecule, and there was competitive adsorption between H_2O and NO_x. Consequently, it could be inferred that for the HPW/SnO_2 system, the characteristic peak at 2266 cm^{-1} should also be created by the NOH^+ vibration entering the HPW secondary structure. The interaction between SnO_2 and HPW was correspondingly small and did not cause changes in the HPW structure. HPW with a pseudo liquid phase acted as the main component for NO_x adsorption, and SnO_2 acted as a catalyst assistant. In the presence of O_2 and H_2O, NO_x could be adsorbed on the surface of the HPW or further into its bulk phase to replace part of the crystal water in the secondary HPW structure, where, finally, adsorbed NO_x existed in the catalyst in the form of NOH^+.

3.7 Catalytic Decomposition of Adsorbed NO_x

Catalytic decomposition products of adsorbed NO_x on HPW and HPW/SnO_2 was detected using GC-MS. N_2 was found in the products, for which the obtained results are shown in Fig. 7. For HPW, N_2 formation was detected 2 min after the start of the increase in the temperature, and a N_2 peak was detected around 8 min later. The decomposition basically ended after 16 min. For HPW/SnO_2, the detected N_2 reached a peak in about 14 min, and the decomposition was basically completed

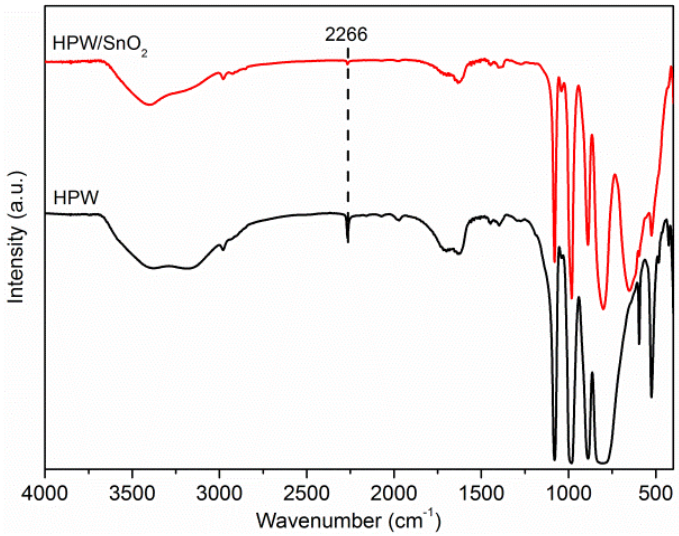

Fig. 6. FTIR of HPW and HPW/SnO_2 (50% loading) after adsorption saturation.

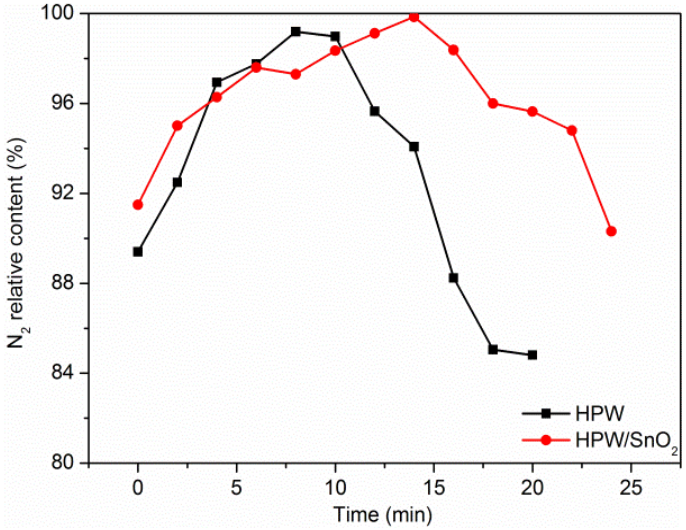

Fig. 7. Catalytic decomposition of adsorbed NO_x on HPW and HPW/SnO_2 (50% loading).

in about 24 min. The experimental results showed that the decomposition time of HPW/SnO_2 with the 50% loading was longer than that for HPW, so it can be reasonably concluded that the addition of the SnO_2 support was not only beneficial to the NO_x adsorption performance, but the combination also contributed to improving the efficiency of NO conversion, thereby leading to more N_2 conversion. The used catalyst could be regenerated by placing it in humid air (5% water vapor) below 100°C, where HPW can replenish the lattice water replaced by NO_x by adsorbing water molecules. Therefore, the new NO_x adsorption-decomposition system screened in this work can achieve NO_x to N_2 without the use of reducing agents.

4 CONCLUSIONS

In summary, several new catalyst systems, different HPAs, and supported HPWs (HPW/SiO_2, HPW/SnO_2, HPW/USY and HPW/ZSM-5) were prepared and used for the adsorption and decomposition of NO_x. The results showed that W-containing HPAs were superior to Mo-containing HPAs. Among the selected catalysts, HPW/SnO_2 with a 50% HPW loading had the highest NO_x adsorption rate of 77.3%, and its saturated NO_x adsorption amount (85.4 mg g^{-1}) was much higher than that of HPW (50.5 mg g^{-1}). With HPW as the main active component, the interaction between HPW and the support affected the HPW properties, in turn affecting its NO_x adsorption performance. When the interaction was stronger, the adsorption rate of the catalyst tended to become lower. The adsorbed NO_x mainly existed in the HPW bulk phase in the form of NOH^+. The GC-MS detection confirmed that the adsorbed NO_x can be decomposed to N_2 using a temperature programming process. This study provides a new experimental basis for which to find a new multi-functional NO_x catalytic decomposition system.

ACKNOWLEDGEMENTS

This work was supported by the National Natural Science Foundation of China [No. 20776080, 20911120088] and the Scientific Innovation program of Shenzhen city, China, under basic research program (JCYJ20170818102915033).

REFERENCES

Abello, L., Bochu, B., Gaskov, A., Koudryavtseva, S., Lucazeau, G., Roumyantseva, M. (1998). Structural characterization of nanocrystalline SnO_2 by X-ray and raman spectroscopy. J. Solid State Chem. 135, 78–85. https://doi.org/10.1006/jssc.1997.7596

Belanger, R., Moffat, J.B. (1995). A comparative study of the adsorption and reaction of nitrogen oxides on 12-Tungstophosphoric, 12-Tungstosilicic, and 12-Molybdophosphoric acids. J. Catal. 152, 179–188. https://doi.org/10.1006/jcat.1995.1071

Chen, N., Yang, R.T. (1995). Activation of nitric oxide by heteropoly compounds: Structure of nitric-oxide linkages in tungstophosphoric acid with keggin units. J. Catal. 157, 76–86. https://doi.org/10.1006/jcat.1995.1269

Forzatti, P., Nova, I., Tronconi, E. (2009). Enhanced NH_3 selective catalytic reduction for NO_x abatement. Angew. Chem. Int. Edit. 48, 8366–8368. https://doi.org/10.1002/anie.200903857

Gómez-García, M.A., Pitchon, V., Kiennemann, A. (2005a). Removal of NO_x from lean exhaust gas by storage/reduction on $H_3PW_{12}O_{40}{\cdot}6H_2O$ supported on $Ce_xZr_{4-x}O_8$. Environ. Sci. Technol. 39, 638–644. https://doi.org/10.1021/es0498641

Gómez-García, M.A., Pitchon, V., Kiennemann, A. (2005b). Storage and reduction of lean–NO_x by using $H_3PW_{12}O_{40}{\cdot}6H_2O$ supported on $Ti_xZr_{1-x}O_4$. Catal. Today 107–108, 60–67. https://doi.org/10.1016/j.cattod.2005.07.164

Hamad, H., Soulard, M., Lebeau, B., Patarin, J., Hamieh, T., Toufaily, J., Mahzoul, H. (2007). A new way for deNO_x catalyst preparation: Direct incorporation of 12-tungstophosphoric acid $H_3PW_{12}O_{40}$ and platinum into mesoporous molecular sieves material. J. Mol. Catal. A: Chem. 278, 53–63. https://doi.org/10.1016/j.molcata.2007.08.024

Herring, A.M., McCormick, R.L. (1998). In situ infrared study of the absorption of nitric oxide by 12-tungstophosphoric acid. J. Phys. Chem. B 102, 3175–3184. https://doi.org/10.1021/jp9727660

Herring, A.M., Mccormick, R.L., Boonrueng, S.R. (2000). A comparison of the interaction of nitric oxide with the heteropolytungstic acids $H_3PW_{12}O_{40}$, $H_{0.5}Cs_{2.5}PW_{12}O_{40}$, $HMgPW_{12}O_{40}$, $H_8SiW_{11}O_{38}$, $H_4SiW_{12}O_{40}$, and $H_{10}CoW_{12}O_{42}$. J. Physi. Chem. B 104, 4653–4660. https://doi.org/10.1021/jp9938213

Hodjati, S., Vaezzadeh, K., Petit, C., Pitchon, V., Kiennemann, A. (2001). The mechanism of the selective NO_x sorption on $H_3PW_{12}O_{40}{\cdot}6H_2O$ (HPW). Top. Catal. 16–17, 151–155. https://doi.org/10.1023/A:1016655519790

Huang, Y., Su, W., Wang, R., Zhao, T. (2019). Removal of typical industrial gaseous pollutants: From carbon, zeolite, and metal-organic frameworks to molecularly imprinted adsorbents. Aerosol Air Qual. Res. 19, 2130–2150. https://doi.org/10.4209/aaqr.2019.04.0215

Imanaka, N., Masui, T. (2012). Advances in direct NO_x decomposition catalysts. Appl. Catal., A 431–432, 1–8. https://doi.org/10.1016/j.apcata.2012.02.047

Jiang, H., Wang, Q., Wang, H., Chen, Y., Zhang, M. (2016). MOF-74 as an efficient catalyst for the low-temperature selective catalytic reduction of NO_x with NH_3. ACS Appl. Mater. Interfaces 8, 26817–26826. https://doi.org/10.1021/acsami.6b08851

Jozefowicz, L.C., Karge, H.G., Vasilyeva, E., Moffat, J.B. (1993). A microcalorimetric investigation of heteropolyacids. Microporous Mater. 1, 313–322. https://doi.org/10.1016/0927-6513(93)80047-X

Konsolakis, M. (2015). Recent advances on nitrous oxide (N_2O) decomposition over non-noble metal oxide catalysts: Catalytic performance, mechanistic considerations and surface chemistry aspects. ACS Catal. 5, 6397–6421. https://doi.org/10.1021/acscatal.5b01605

Liu, F., Yu, Y., He, H. (2014). Environmentally-benign catalysts for the selective catalytic reduction of NO_x from diesel engines: Structure–activity relationship and reaction mechanism aspects. Chem. Commun. 50, 8445. https://doi.org/10.1039/c4cc01098a

Liu, Q., Wu, W., Wang, Y., Wang, J. (2003). Preparation, characterization and catalytic behavior of heteropoly acid immobilized on ultra stable Y zeolite I. Preparation and characterization. Petrochem. Technol. 32, 387–391. https://doi.org/10.3321/j.issn:1000-8144.2003.05.007

Mccormick, R.L., Boonrueng, S.K., Herring, A.M. (1998). In situ IR and temperature programmed desorption-mass spectrometry study of NO absorption and decomposition by silica supported 12-tungstophosphoric acid. Catal. Today 42, 145–157. https://doi.org/10.1016/S0920-5861(98)00085-6

Munir, D., Usman., M.R. (2018). Catalytic hydropyrolysis of a model municipal waste plastic mixture over composite USY/SBA-16 catalysts. J. Anal. Appl. Pyrol. 135, 44–53. https://doi.org/10.1016/j.jaap.2018.09.023

On, D.T., Kaliaguine, S., Bonneviot, L. (1995). Titanium boralites with MFI structure characterized

using XRD, XANES, IR, and UV-visible techniques: Effect of hydrogen peroxide on the preparation. J. Catal. 157, 235–243. https://doi.org/10.1006/jcat.1995.1284

Ren, Z., Fan, H., Wang, R. (2017a). A novel ring-like Fe_2O_3-based catalyst: Tungstophosphoric acid modification, NH_3-SCR activity and tolerance to H_2O and SO_2. Catal. Commun. 100, 71–75. https://doi.org/10.1016/j.catcom.2017.06.038

Ren, Z., Teng, Y., Wang, R. (2017b). Keggin-tungstophosphoric acid decorated Fe_2O_3 nanoring as a new catalyst for selective catalytic reduction of NO_x with ammonia. Catal. Today 297, 36–45. https://doi.org/10.1016/j.cattod.2017.06.036

Rocchiccioli-Deltcheff, C., Amirouche, M., Hervé, G., Fournier, M., Che, M., Tatibouet, J.M. (2010). Structure and catalytic properties of silica-supported polyoxomolybdates: II. Thermal Behavior of Unsupported and Silica-Supported 12-Molybdosilicic Acid catalysts from IR and Catalytic Reactivity Studies. J. Catal. 126, 591–599. https://doi.org/10.1016/0021-9517(90)90022-C

Shen, B., Wu, C., Guo, B., Wang, R., Liang, C. (2007). Pyrolysis of waste tyres with zeolite USY and ZSM-5 catalysts. Appl. Catal., B 73, 150–157. https://doi.org/10.1016/j.apcatb.2006.07.006

Shirazi, L., Jamshidi, E., Ghasemi, M.R. (2008). The effect of Si/Al ratio of ZSM-5 zeolite on its morphology, acidity and crystal size. Cryst. Res. Technol. 43, 1300–1306. https://doi.org/10.1002/crat.200800149

Singh, L.P., Luwang, M.N., Srivastava, S.K. (2014). Luminescence and photocatalytic studies of Sm^{3+} ion doped SnO_2 nanoparticles. New J. Chem. 38, 115–121. https://doi.org/10.1039/C3NJ00759F

Sun Q., Wang, Z., Wang, D., Hong, Z., Zhou, M., Li, X. (2018). A review on the catalytic decomposition of NO to N_2 and O_2: Catalysts and processes. Catal. Sci. Technol. 8, 4563–4575. https://doi.org/10.1039/C8CY01114A

Wang, R., Zhang, X., Ren, Z. (2021). Germanium-based polyoxometalates for the adsorption-decomposition of NO_x. J. Hazard. Mater. 402, 123494. https://doi.org/10.1016/j.jhazmat.2020.123494

Wang, S., Yang, G. (2015). Recent advances in polyoxometalate-catalyzed reactions. Chem. Rev. 115, 4893–4962. https://doi.org/10.1021/cr500390v

Wu, J., Jin, S., Wei, X., Gu, F., Han, Q., Lan, Y., Qian, C., Li, J., Wang, X., Zhang, R., Qiao, W., Liang, L., Jin, M. (2021). Enhanced sulfur resistance of $H_3PW_{12}O_{40}$-modified Fe_2O_3 catalyst for NH_3-SCR: Synergistic effect of surface acidity and oxidation ability. Chem. Engin. J. 412, 128712. https://doi.org/10.1016/j.cej.2021.128712

Yang, R.T., Chen, N. (1994). A new approach to decomposition of nitric oxide using sorbent/catalyst without reducing gas: Use of heteropoly compounds. Ind. Eng. Chem. Res. 33, 825–831. https://doi.org/10.1021/ie00028a007

Zhang, X., Cheng, L., Yang, F., Wang, R., Vladimir, K. (2012). NO_x adsorption and decomposition over $H_3PW_{12}O_{40}$/CNTs and the effect of microwave irradiation. Chem. J. Chin. Univ. 33, 1826–1834. https://doi.org/10.3969/j.issn.0251-0790.2012.08.035

Zhang, X., Wang, R. (2013). Preparation, characterization and NO_x catalytic decomposition behavior of ship-in-bottle type $H_3PW_{12}O_{40}$-NaY catalyst. Chin. J. Inorg. Chem. 29, 249–256. https://doi.org/10.3969/j.issn.1001-4861.2013.00.074

Zhang, Z., Han, Y., Zhu, L., Wang, R., Yu, Y., Qiu, S., Zhao, D., Xiao, F. (2001). Strongly acidic and high-temperature hydrothermally stable mesoporous aluminosilicates with ordered hexagonal structure. Angew. Chem. Int. Edit. 40, 1258–1262. https://doi.org/10.1002/1521-3773(20010401)40:7<1258::AID-ANIE1258>3.0.CO;2-C

Zhang, Z., Zhu, L., Ma, J., Ren, S., Yang, X. (2002). Temperature programmed desorption-mass spectrometry study of NO desorption and decomposition by titania supported 12-tungstophosphoric acid. React. Kinet. Catal. Lett. 76, 93–101. https://doi.org/10.1023/A:1015669529142